Chapter 1 – INTRODUCTION

Small slow-flying objects are likely to be subjected to combination of severe unsteadiness and flow separation. The flight vehicle is likely to find itself at high angle of attack, or to rapidly change angle of attack, or to be influenced by winds, such that angles of attack would be large, and quickly varying. High frequencies and maneuver-amplitudes do not occur for lumbering transport aircraft or even for missiles or maneuvering fighters, where the reduced-frequencies are low because the flight speed is high and convective time (ratio of wing mean aerodynamic chord to flight speed) is fast. The so-called "Micro Air Vehicles", or MAVs, spawned interest in basic questions of unsteadiness and massive separation at high frequency, and for these problems low Reynolds number is concomitant, simply from the scales of fluid density, kinematic viscosity, frequency and amplitude of motion.

We focus on what happens when an abstracted body – a rigid flat plate – accelerates with respect to a fluid. We do not address specific applications or the design of MAVs, or motivating flight modalities in nature. These are extensive and deeply interesting topics, where unsteady aerodynamics is of great relevance. Indeed, the problem of how flapping-wing insects generate high stroke-averaged lift coefficients (see for example [1]) has been the motivation for prior STO AVT Task Groups, such as AVT-149 [2], and continues to inform the question of how lift is connected with wing geometry, flapping kinematics, Reynolds number and so forth. Operation at small Reynolds number seems to necessitate unsteady lift mechanisms to produce acceptably high lift coefficients; see for example the taxonomy in Figure 1-1. However, the present objective is to elucidate a small but expository set of abstract problems, and to connect flowfield phenomena to aerodynamic force history, and perhaps thenceforth to build a reduced-order model that might ultimately be useful for engineers. For problems that are highly unsteady, to what extent does the resulting aerodynamic response significantly differ from the nominal steady values? The present work is concerned with unsteady aerodynamics, where flow separation is massive, and there is non-trivial coupling between flow separation from bluff-body effects (alternatively from deep stall of streamlined shapes) and from the imposed motion. The problem is taken as being identically incompressible, even though applications of dynamic stall such as helicopter rotors are of course strongly influenced by compressibility [12].

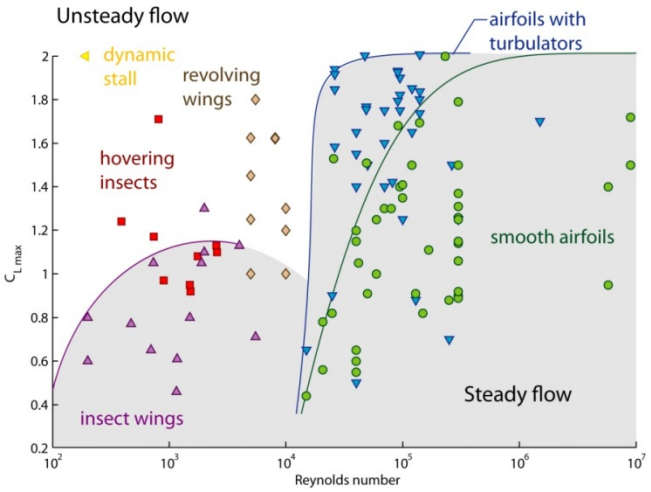

Figure 1-1: Notional Scatter-Plot of Maximum Lift Coefficient vs. Reynolds Number for a Range of Operating Conditions, Citing in Particular the Utility of Unsteady Mechanisms for High-Lift Production at Very Low Re, where Purely Steady Means Result in Unacceptable Paucity of Lift. After Jones [28].

The limit of high frequency and low amplitude has been rationalized over 70 years ago, mainly in the context of aeroelasticity, using potential-flow assumptions [3]. The outcome was Theodorsen's celebrated formula and its various extensions and reformulations. Though such formulas were shown to be valid predictors of lift-history even for some aggressive motions where the underlying assumptions of attached-flow and planar-wake are falsified [4], such pleasant conclusion is not universal [5], especially for large-amplitude motions. We therefore need to understand the impact of flow separation, or more properly, of vortices shed from the plate's leading and trailing edges, and how these cause departure from the predictions of attached-flow theory. This, in essence, is the focus of our Task Group.

Unsteady problems begin with a definition of kinematics. Next, we cover facilities and methods, give a resume of computations and measurements, and finally present an analytical/phenomenological conjecture and its corroboration by the data.

1.1 RESUME OF KINEMATICS

In 2D, a flat plate can pitch about some pivot point, plunge (move normal to the relative free-stream direction) and surge (move parallel to the free-stream direction). Thus there are three degrees of freedom, plus the various kinematic conditions: pitch pivot point, initial incidence, final incidence, reduced frequency, plunge amplitude, and surge amplitude. "Normal hover" [6] is a form of combined pitch/plunge, where the absence of a free-stream confounds the usual definitions of reduced frequency and Reynolds number. Another special case is pure surge in a fluid quiescent in the lab frame, where the plate begins at rest and accelerates through some motion-profile, typically at some fixed incidence angle, reaching a steady free-stream.

3D introduces a bewildering plethora of additional kinematic possibilities. Now the wing has finite span, with inboard and outboard wingtips. Most important is rotation about some fixed point near the inboard tip, typically located some chord-fraction outside the wing. Roll of the wing (in some conventions called "flapping") is not considered here, as we regard it as derivative of 2D plunge. Yaw is a form of rotation, and spanwise translation is irrelevant.

In 3D the wing is always finite-span, and four kinds of motion are possible:

- Rectilinear translation in surge;
- Rectilinear pitch, meaning a pitch about a spanwise-aligned axis, in steady free-stream;
- Rotational surge about a fixed point near the inboard wingtip, with constant incidence angle of the plate; and
- Combination of rotation with pitch, where the rotation is a fixed speed but the incidence angle is ramped up.

The key comparisons are rotation vs. translation, and surge vs. pitch. Mediating the four principal kinds of motion are Reynolds number, reduced frequency and aspect ratio of the plate. A schematic rendition of the four principal cases and associated secondary considerations is given in Figure 1-2. Reduced frequency for transient motions is:

$$K = \frac{\dot{\theta} c}{2U_\infty} \qquad \text{(Eq. 1-1)}$$

where "f" is the frequency, "c" the chord of the plate, and the denominator is twice the relative-free-stream steady speed. "K" is therefore just a convective normalization of the dimensional pitch rate.

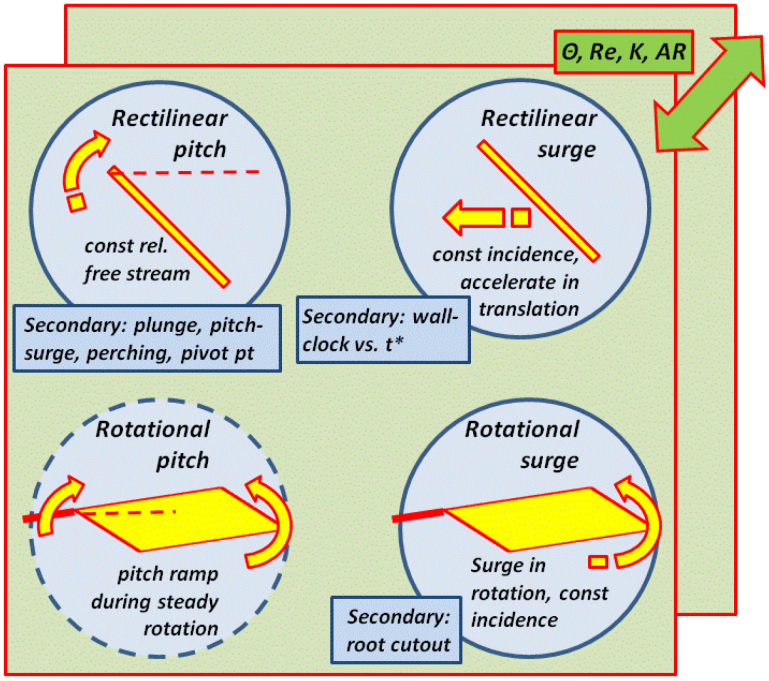

Figure 1-2: Schematic of the Four Prime Test Conditions. Reynolds number, peak incidence angle, reduced frequency, pitch pivot-point, plate aspect ratio and leading edge shape, and rotating-plate root cut-out are additional parameters pursued by some groups. For all four kinds of motion, the "fast case" has the acceleration occurring over one chord (surge from rest to steady towing-speed over one chord, pitch from zero incidence to 45-degrees over one convective-time in a steady free stream), and the "slow case" occurs over 6 chords. Thus there are 8 total principal cases.

Details of kinematics – velocity profiles and time-base – are given in Figure 1-3. Note that for problems without a lab-frame steady free stream, where the test article starts from rest, there are two alternatives to defining the running time-base, either the wall-clock (seconds), or a 'convective time' where the distance travelled by the leading edge of the wing is made dimensionless by chord-length. These are unimportant and almost fungible for the long-term history, but can be important for force transients at high-rate and early time. The incidence-angle history in Figure 1-3 is a linear ramp with smoothed "corners". Smoothing is via a C^{∞} rational-function, $\hat{G}(t/T)$, proposed by Eldredge *et al*. [7]:

$$G(t/T) = \ln[(\cosh(A)\cosh(D))/\cosh(B)\cosh(C)],$$

$$A = 2a(\frac{2\pi t}{T} + \frac{2-\pi}{2}),$$

$$B = 2a(\frac{2\pi t}{T} - \frac{2+\pi}{2}), \qquad \text{(Eq. 1-2)}$$

$$C = 2a(\frac{2\pi t}{T} + \frac{2-3\pi}{2}),$$

$$D = 2a(\frac{2\pi t}{T} - \frac{2+3\pi}{2}),$$

$$\hat{G}(t/T) = h_0(1 - 2G(t/T)/max(G)) \ .$$

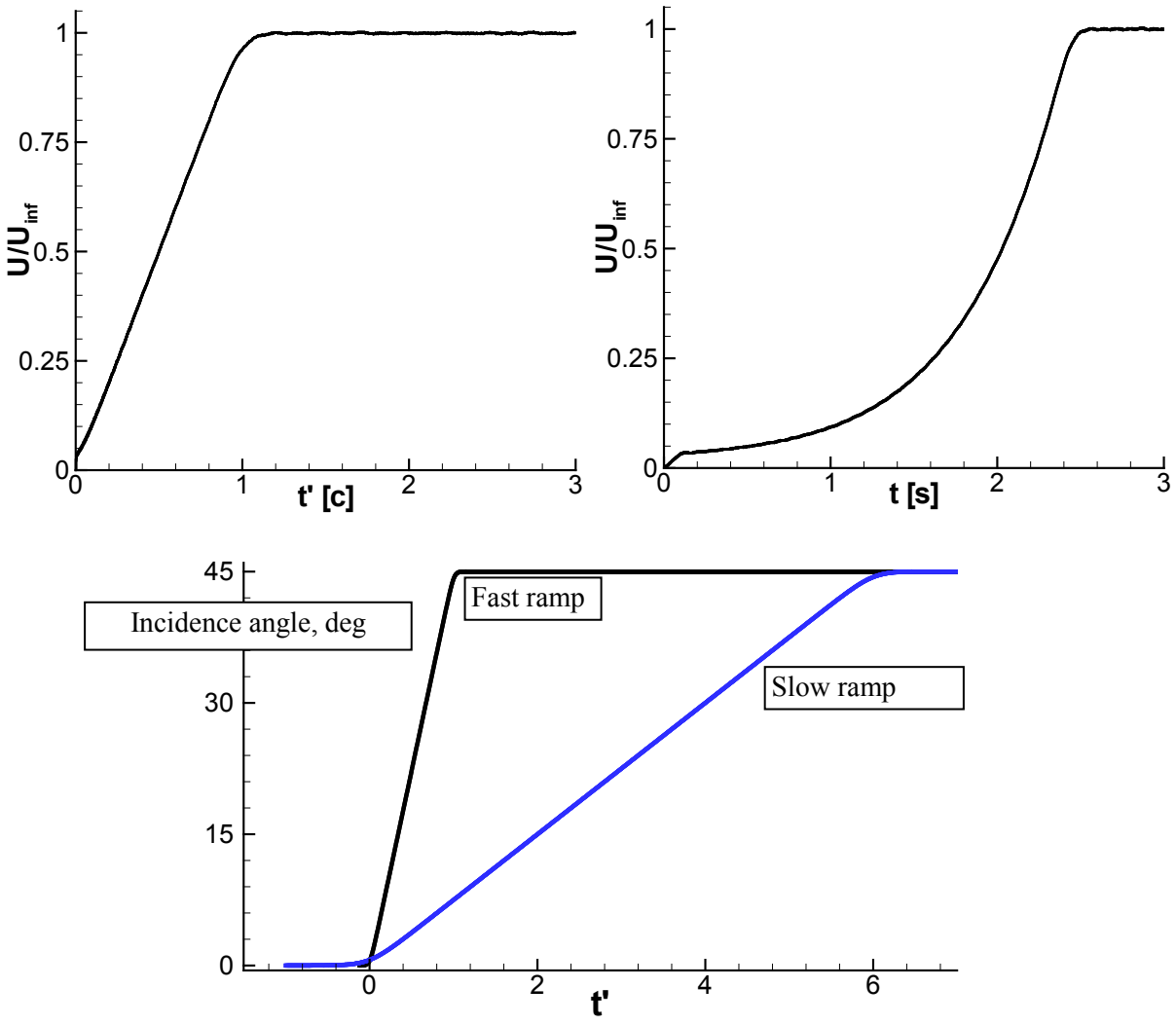

Figure 1-3: Typical Velocity Histories. Top row: Smoothed ramp in surging velocity, passing from initial condition (at rest) to final condition (normalized value of 1); ramp in velocity linear with convective time (left) looks like an exponential when plotted vs. wall-clock time in seconds (right). The distinction between the two causes a difference in force history during the acceleration, which enervates almost immediately upon cessation of acceleration. Bottom row: "Slow" ramp (blue, 6 convective times, or K = π/48) and "fast" ramp (black, 1 convective time, or K = π/8) in pitch, starting from θ = 0° and concluding with θ = 45°. In pitch, there is a constant free-stream, so linear ramps with respect to wall-clock or convective time are equivalent.

The function *G(t/T)* has four non-dimensional-time parameters (*A*, *B*, *C* and *D* in Eq. 2), one each at the "corner" of the trapezoidal motion profile. The parameter "*a*", which controls the amount of smoothing, is a dimensionless acceleration upper bound, typically limited by mechanical acceleration of a laboratory apparatus. The $\hat{G}(t/T)$ function can be applied to transient or periodic motions, the latter looking like a smoothed sawtooth train.

AVT-202 cases are primarily of aspect ratio AR = 2 (rotational motions) and AR = 4 (rectilinear motions), the reasoning being that in rotation there is one "blade" of two, each blade of AR = 2.

Much today is made of PIV post-processing to assess vortex strength and to calculated integrated aerodynamic loads from the flowfield [8]. Our approach does not pursue whole-field velocity/vorticity integration for arriving at aerodynamic force history, but instead to advocate for a phenomenological model, tracking a small number (ideally, just two) discrete vortices. An important recent advance was the vortex-recognition method of Graftieaux [9], enabling:

1) Assessing for whether a given flowfield structure is a credible vortex; and
2) How to define its boundary to calculate circulation by integrating vorticity within this boundary.

We follow this approach to extract LEV and TEV circulation strength evolution, and vortex-core trajectory as a function of plate displacement.

The motions in Figure 1-2 and Figure 1-3 are all transient: they begin from some initial condition, either with no relative motion between the body and the ambient fluid, or with the body in a zero-lift condition (zero incidence for an uncambered plate) in a steady flow. They pass through a transient and arrive again at the same nominal steady-state condition, where relative acceleration between body and fluid ceases, though bluff-body shedding can result in a perpetually unsteady flow. The complementary case, not examined in AVT-202, is that of periodic motion, where the body executes some trajectory that repeats itself with a characteristic frequency. We consider transient motions, as opposed to periodic motions, because lags/transients are obvious in the remaining aerodynamic response after the motion has ceased, and are not inherited in the following period, as they would be in periodic motions. There is explicitly a phase of motion where acceleration is non-zero, followed by a long (ideally infinite) run where the relative free-stream is steady. For the rotating plates, after completing a full revolution the plate enters its own wake, and in that narrow sense the resulting flow remains unsteady. The end-state of all motions is deep-stall, typically at 45 degrees incidence.

1.2 PRINCIPAL SCIENTIFIC QUESTIONS OF THIS STUDY

Our interest includes the following questions:

1) Why do so many disparate geometries, motions and resulting flowfields evince similar aerodynamic force histories? Is there a unifying principle, and perhaps a low-order modeling scheme, accounting for this?
2) What is the budget of circulatory and non-circulatory load-contributions while the plate is accelerating? Can these respective contributions be linearly superimposed, to form the total aerodynamic force history? How much of the lift budget is carried by the LEV, TEV, bound circulation (including pitch-rate effects)?
3) What are the long-term transients (residual unsteadiness in the aerodynamic response and the flowfield) after the motion has completed? That is, to what extent does the accelerating portion of the motion affect vortex history (and loads history)?
4) What are criteria for vortex initiation, saturation, and detachment? Are there multiple vortices at the LE after the initial LEV? Are there multiple vortices at the TE after the starting-vortex has been ejected?
5) How does aerodynamic force production scale with pitch rate, pitch pivot point location and peak incidence angle? Is there a fundamental difference in lift-production between rotation and translation, between pitch and surge?
6) Are 3D structures important in the vortex topology? Do finite-aspect-ratio wings evince fundamentally different integrated aerodynamic load histories than those in 2D? How do tip vortices mediate LEV/

TEV production and bound circulation? More broadly, what sort of spanwise variations are there for low and moderate aspect ratio wings?

7) How does Reynolds number mediate vortex production/evolution, and aerodynamic force history?

1.3 BRIEF REVIEW OF CLASSICAL ANALYTICAL MODELS

Wagner [53] was one of the earliest researchers to study the lift generated by an airfoil starting from rest at a small fixed angle of attack, in this case for impulsive start, where the acceleration in surge is infinitely large, occurring over infinitesimal time. Clearly the application of Wagner's model to AVT-202 cases (all of which have finite acceleration over finite time) requires some discretion. Based on the physical assumption that the velocity at the trailing edge is always finite and by modeling the wake as a flat vortex sheet, Wagner was able to determine the lift as a function of chords travelled. At any point, Wagner assumed that the circulatory lift was produced by a bound circulation in accordance with thin airfoil theory that is in the absence of separation. Non-circulatory lift is just a delta function. Wagner's analysis shows that the effective angle of attack is reduced due to the downwash from the shed vortices in the wake. This in turn delays the build-up of the bound circulation, which leads to further shedding of vortices in the wake and as a result there is a considerable delay in the development of the ultimate steady-state lift. Figure 1-4 (from Wagner [53]) compares the growth of lift with the growth of circulation. Half of the final lift is assumed at once, and the lift then gradually approaches its steady asymptote. The circulation, however, rises steadily from zero.

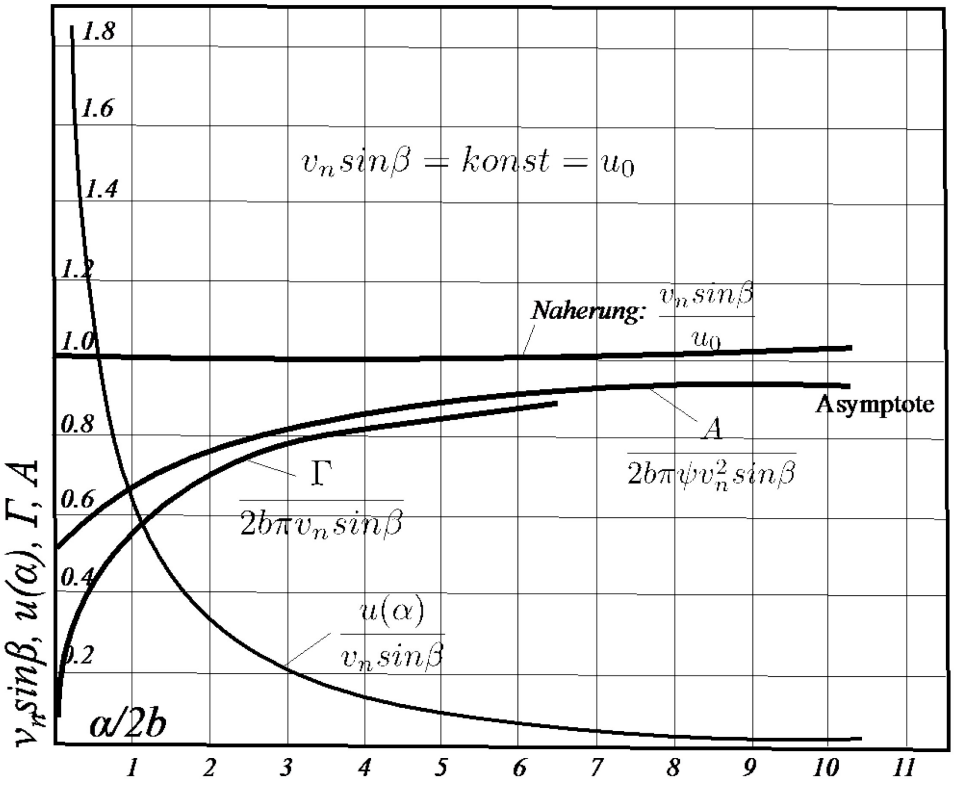

Figure 1-4: Wagner's Lift Prediction (marked 'A', starting at 0.5) and Rendition of Wagner's Bound Circulation Γ Starting from Zero. Note that the "Wagner function" is typically taken to begin from 0.5. [53].

1.4 REDUCED-ORDER MODEL OF VORTEX PHYSICS

One of the chief aims of this Report is to propose and to experimentally corroborate a simple semi-analytical scheme to predict the unsteady lift generated by a flat plate in an unsteady flow in two dimensions. All of the "canonical" cases in this Report are plates of finite aspect ratio, whence a 2D model cannot be physically accurate, especially considering the role of tip vortices for translational cases and radial-effects in LEV stabilization for the rotational cases. Nevertheless, a 2D simplification, for example in a strip-theory sense, is eminently attractive. Accordingly, here we consider a flat plate accelerating from rest at a constant angle of attack, and a flat plate pitching in a steady free-stream. The treatment is inviscid and incompressible.

1.4.1 Non-Circulatory and Circulatory Force Contributions

We postulate that the unsteady force exerted by an object onto the surrounding fluid (and thus the opposite reaction force experienced by the object) is equal to the rate of change of momentum in the surrounding fluid. To quantify this force it is necessary to integrate the momentum across the whole flowfield (stretching to infinity) and then take the time derivative[1]:

$$F = \frac{d}{dt} \iint_{-\infty}^{\infty} \rho \, \boldsymbol{u}(\boldsymbol{x}, t) \, dA$$

where $\boldsymbol{u}$ is the unsteady velocity field, $\boldsymbol{x}$ is the location vector, t is time and A is an area element ($dxdy$). Thus, if it were possible to accurately determine the velocity field everywhere at several instances in time, one could determine the force experienced by an object – e.g., lift and drag. In reality however, there are practical difficulties making this untenable.

An important simplification is possible for situations where the unsteady flow around an object is self-similar. By this we mean a flowfield topology (streamline pattern) that is independent of time, although the magnitude of local velocity may scale with a time-varying free-stream $U_\infty(t)$:

$$\boldsymbol{u}(\boldsymbol{x}, t) = \boldsymbol{U}_\infty(t) \, k(\boldsymbol{x})$$

Here $k(\boldsymbol{x})$ is some function relating the local velocity to the (variable) free stream. Note that k is constant in time. Thus, the force experienced by the object can be expressed as:

$$\boldsymbol{F} = \underbrace{\rho \iint_{-\infty}^{\infty} k(\boldsymbol{x}) dA}_{I} \underbrace{\frac{dU_\infty(t)}{dt}}_{II}$$

The force is therefore the product of a time-invariant area integral of $k(\boldsymbol{x})$ (Term I) and the acceleration of the free-stream (Term II). Note that the first term (I) has the unit of mass, and is constant throughout the motion. The force is proportional to the acceleration, and hence the term 'virtual mass' or 'added mass'[2].

[1] Here, it is implied that the pressure is uniform at the integration boundary (∞). Vector quantities are in bold.

[2] Though other treatments are possible, one could go further and declare any attempt to make the calculation of virtual mass force "more accurate" futile because such an approach tries to more closely approximate the real momentum change of the surrounding fluid. Taken to the extreme, this "virtual mass force" would eventually be equivalent to the total force experienced by the flow (first equation).

An expository case for considering this force contribution is the classical potential flow around an accelerating flat plate at 90° angle of attack (Figure 1-5).

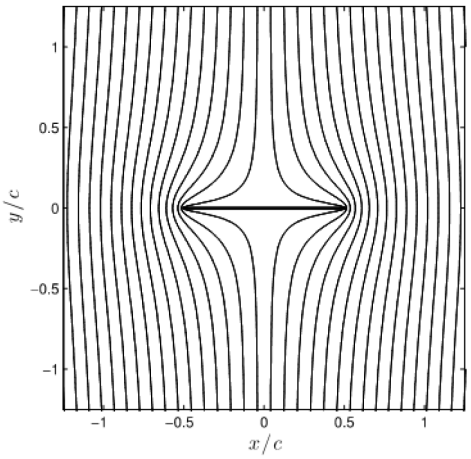

Figure 1-5: Potential Flow Around a Flat Plate at 90° Angle of Attack.

In steady potential flow, the plate experiences identically zero force. However, in unsteady flow the surface pressures on the windward side are increased, while the pressures on the leeward side are decreased (e.g., unsteady Bernoulli equation), giving a net force:

$$F = \frac{\rho c^2 \pi}{4} \dot{V}$$

where c is the chord of the plate and V the plate-normal velocity of the fluid. This force is exactly equivalent to the inertia of a circular cylinder of fluid with diameter c undergoing the same motion as the plate. For a plate accelerating at an angle of attack, only the velocity component normal to the plate contributes to this force (by the principle of superposition and assuming the flow to remain inviscid, i.e., attached).

Realistic flows are not self-similar, and viscous forces are not negligible. We thus postulate that the total unsteady force is the sum of the added mass force and a second circulatory force contribution [3]. We shall persist with the contrivance of inviscid flow to determine the added-mass term by considering the plate-normal velocity at mid-chord and equating the force to the added mass force experienced in potential flow of a flat plate at 90° angle of attack.

We next turn to the circulatory contribution. The simplest model for a circulatory force is to consider the relationship between forces and vortices. The flow shown in Figure 1-6 has a net momentum, thus the generation of a pair of vortices (of equal but opposite strengths) in a quiescent fluid requires a force (by force-momentum equation). According to Lamb [10], the magnitude of this momentum is:

$$J = \rho d\Gamma$$

[3] Early on in the motion the flow is quite close to the potential flow model and thus the initial force should be reasonably close to the prediction. A much more rigorous treatment actually shows that even in a complex viscous unsteady flow the added mass term remains that seen for the potential flow around the same object, and the total force is indeed the sum of this force and all circulatory (viscous) components.

where J is the impulse (momentum), d the distance between the vortex centroids, and Γ the vortex circulation. Since force equals the rate of change of momentum, the chain rule of differentiation gives:

$$F = \rho(\dot{d}\Gamma + d\dot{\Gamma})$$

(where *dot* signifies time derivatives). This shows that vortex lift has two contributions, one related to strength of vortices and the growth in distance between them (and this term leads to $L = \rho U\Gamma$ in steady flow), and another related to the growth of circulation. The direction of the force is normal to the line connecting the two vortices.

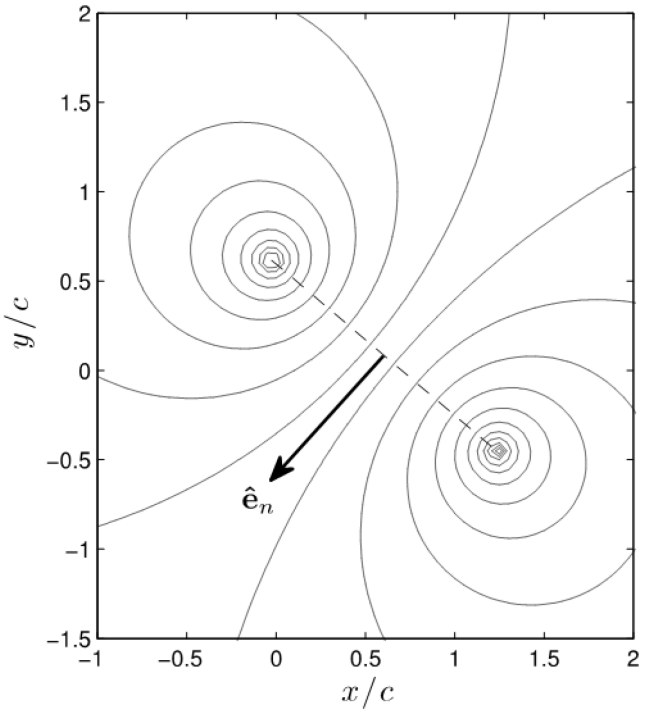

Figure 1-6: Potential Flow Streamlines Around a Stationary Counter-Rotating Vortex Pair. This flow has net momentum produced by the vortex pair, and therefore results in a net force.

Let us consider a flat plate in unsteady flow as being the source of such a force through the generation of a starting vortex (or TEV), and either bound circulation or a LEV associable with the plate. Setting x as the streamwise co-ordinate, lift is the y-component of this force. Knowledge of the strengths and positions of the two vortices (LEV and TEV) allows us to compute this circulatory lift force and to express it in coefficient form (where u_i are the x-components of vortex velocities, and x_i are the x-components of vortex locations):

$$C_{l,circ} = -\frac{2}{U_\infty^2 c}\left[(u_{LEV} - u_{TEV})\Gamma_{LEV} + (x_{LEV} - x_{TEV})\dot{\Gamma}_{LEV}\right]$$

Note that this is non-dimensionalised by a free stream velocity U_∞. Apart from the choice of U_∞ and the direction of the lift force, this result is independent of the coordinate system.

In situations where there is both bound circulation and a LEV, it is suggested that we 'lump together' both vortices by calculating the total circulation and a centroid location (like a centre of gravity). Note that the

position of the centroid can move relative to the plate if the LEV convects with respect to the plate. Thus there are only two vortices in the flow, and these must be of equal and opposite strength according to Kelvin's theorem. In reality, as the LEV changes strength, a vortex sheet is shed from the TE, which may not always merge with the TEV (and even if it does this will take time) and thus the above flow is a relatively crude approximation. However, if we assume (reasonably) that the vortex sheet moves away at U_∞ the first term of the above equation remains correct. Furthermore, it can be argued that because any changes in circulation cause shedding at the trailing edge, an approximation for the distance term in the above equation might be the chord length. Thus we propose to alter the above to:

$$C_{l,circ} = -\frac{2}{U_\infty^2 c}\left[(u_{LEV} - u_{TEV})\Gamma_{LEV} + c\dot{\Gamma}_{LEV}\right]$$

This effectively assumes that the distance between two opposing vortices arising from a change in circulation is equal to the chord length.

Although crude, this model is helpful in understanding the magnitude of circulatory lift generated in an unsteady wing flow, by tracking the LEV and TEV (Figure 1-7). The model illustrates nicely when a *detached* LEV contributes to wing lift:

1) While it continues to strengthen, regardless of its position; and
2) While it moves relative to the TEV.

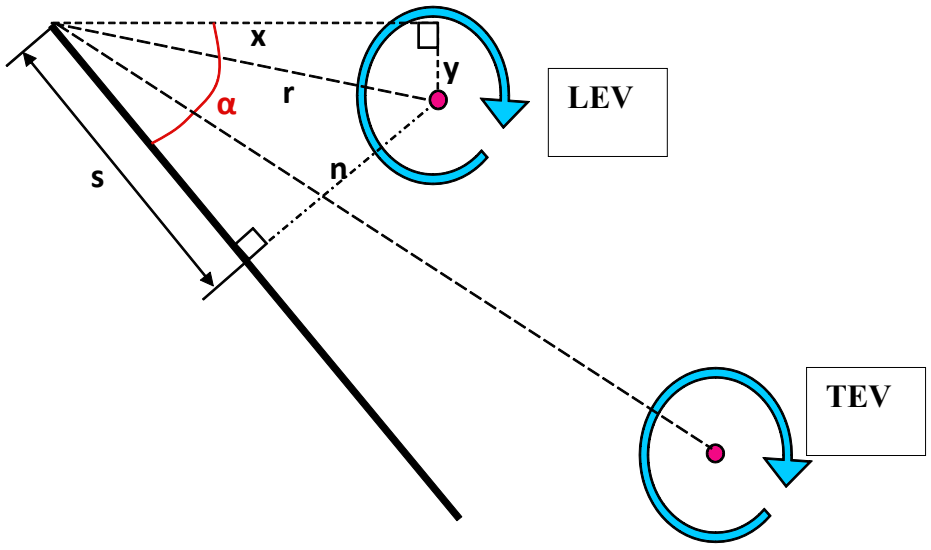

Figure 1-7: Schematic of Leading Edge Vortex (LEV) and Trailing Edge Vortex (TEV) with Respect to the Plate, with Coordinate System with Origin at the Plate's Leading Edge.

Thus, it is not necessary for the LEV to be at a constant position relative to the wing ('*attached*'). As long as it moves away at a slower speed than the TEV (relative to the wing) it contributes to the circulatory force. However, after the LEV is 'shed' it generally stops growing in strength and moves away from the wing at an ever increasing rate, thus reducing its force contribution until it ultimately drifts at free stream velocity, at which point no further force is produced.

With this approach in mind, we proceed to deriving circulatory and non-circulatory lift terms for the surging plate and the pitching plate. As cautionary note, there is no reason why the real viscous flow should be equivalent to the superposition of an accelerating normal flow, a 2-vortex flow and a remaining uniform flow in the direction of the plate. One might compare some PIV flowfields with a flow calculated form this analytical model. In any case, PIV data is necessary to obtain LEV and TEV trajectory history and circulation history.

1.4.2 Analytical Derivations for the Surging Plate

We express the plate-normal velocity as:

$$V = U \sin \alpha$$

The added mass force is:

$$F = \frac{\rho c^2 \pi}{4} \dot{U} \sin \alpha$$

Calculating the component in lift direction:

$$L = F \cos \alpha = \frac{\rho c^2 \pi}{4} \dot{U} \sin \alpha \ \cos \alpha$$

expressed in coefficients this gives:

$$C_{L,non-circ} = \frac{\pi c \dot{U}}{4U^2} \sin 2\alpha$$

No force is generated at vanishing angle of attack. The above result shows that the non-circulatory force is perpendicular to the plate. It is generally more common to normalize the force coefficients in the surging case with the eventual free-stream velocity U_∞. This reduces the lift coefficient during the acceleration phase by $\frac{U(t)}{U_\infty}$.

For the circulatory term, we make use of Pitt-Ford's observation [11] that the bound circulation in surging flat plates tends to vanish early on in the motion. Thus we assume that all circulation in the flow is concentrated in two vortices: an LEV (that need not be attached to the plate) and a TEV. The vorticity shed by changing strength of the LEV is assumed to immediately merge with the TEV. In lieu of PIV data on vortex trajectories and circulations, one could conjecture that Γ_{LEV} grows according to the Wagner function to eventually reach some saturated steady-state value (Figure 1-4). This is not far from the real scenario. We use the Wagner function (starting from zero) rather than the Wagner prediction for lift (which starts at a finite lift coefficient half of the ultimate value) because Wagner assumes that the growth of bound circulation starts from zero. There is no real physical justification of this; it is merely convenient to use this curve because it fits the observed growth of circulation reasonably well as will be shown later in this Report.

Agreement can probably be improved. In the above, the Wagner function was calculated by assuming a constant asymptotic Γ_∞ based on the terminal velocity. If we locally adjust the curve by scaling with $U(t)/U_\infty$ during the acceleration phase, then its shape should fit better with the measured data. The exact Wagner function is iterative, but a close explicit formula is:

$$\frac{\Gamma(t)}{\Gamma_\infty} = 0.914 - 0.3151 \exp\left(\frac{-\frac{s}{c}}{0.1824}\right) - 0.5986 \exp\left(\frac{-\frac{s}{c}}{2.0282}\right)$$

Generally, the steady-state circulation of an LEV is unknown, so we use the equivalent to $2\pi\alpha$. This does not mean that the plate at any point achieves the equivalent value of steady-state lift, because we do not assume that the LEV is perfectly attached to the plate.

We also need an estimate of the LEV motion relative to the plate (or the TEV). As shall be shown in later sections, we can estimate the relative drift velocity between the LEV and the TEV to be between 0.3 and 0.5 of the free stream velocity during the early part of the motion (Figure 1-8). This appears to hold even beyond the acceleration phase, although this cannot be correct indefinitely as the relative velocity eventually has to vanish. To be precise, there appears to be an early stage where the LEV is 'attached', i.e., moving more slowly relative to the wing, but we propose to ignore this because the vortex strength at this stage is still small. Thus the simple $\frac{1}{3}U_\infty$ rule might actually work reasonably well to capture the circulatory force.

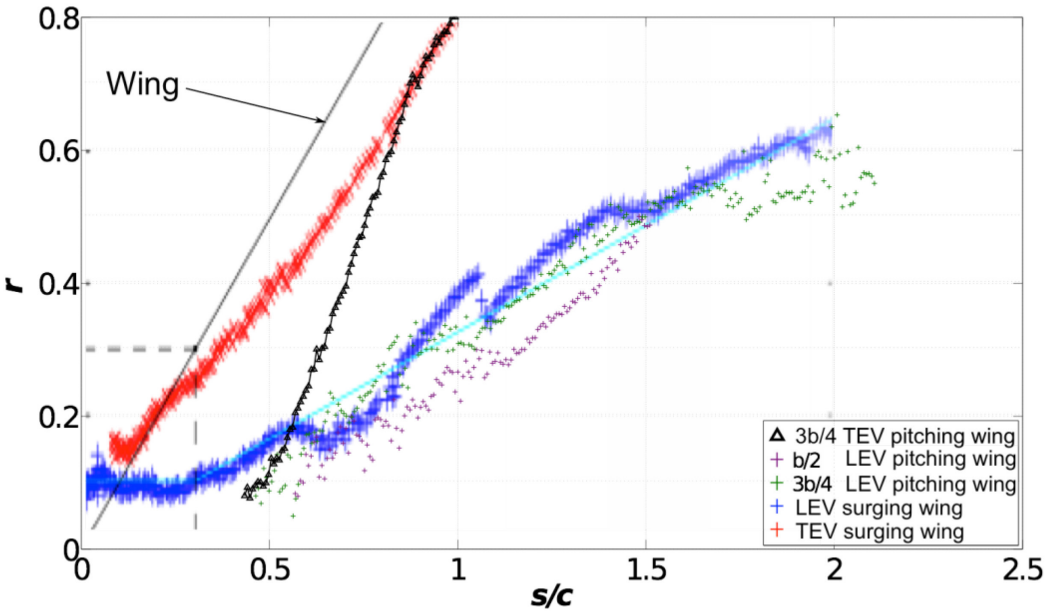

Figure 1-8: Distance of LEV and TEV from the Plate's Leading Edge, Plotted Against Chords-Traveled by the Plate, for the Fast (Once Chord Acceleration) Translational Surging and Pitching Plates.

To summarize, we estimate the unsteady force in the surge case as follows:

1) Add three contributions from virtual mass, vortex growth $\dot{\Gamma}_{LEV}$, and relative LEV/TEV motion.
2) Estimate virtual mass from potential flow result for inclined flat plate. This force occurs during the accelerating portion of the cycle.
3) Estimate the two circulatory contributions by assuming that Γ_{LEV} grows according to the Wagner function with a steady-state value equivalent to $2\pi\alpha$ (most likely Γ_{LEV} is well below this value).

4) Estimate the LEV trajectory by assuming that the distance between the LEV and the TEV grows at 50% of U_∞.

5) Estimate the distance between two vortices used in the $\dot{\Gamma}_{LEV}$ term to equate to chord length c.

6) In each case, non-dimensionalize the result by the asymptotic U_∞ , this may require 'down-scaling' some of the equations given earlier during the accelerating portion of the surge cycle.

At large angles of attack (e.g., 45°) we need to be careful about force directions. The vortex lift acts in a direction normal to the line connecting LEV and TEV, while the non-circulatory force acts normal to the plate. The notional history of lift for the surging plate should then follow the schematic in Figure 1-9.

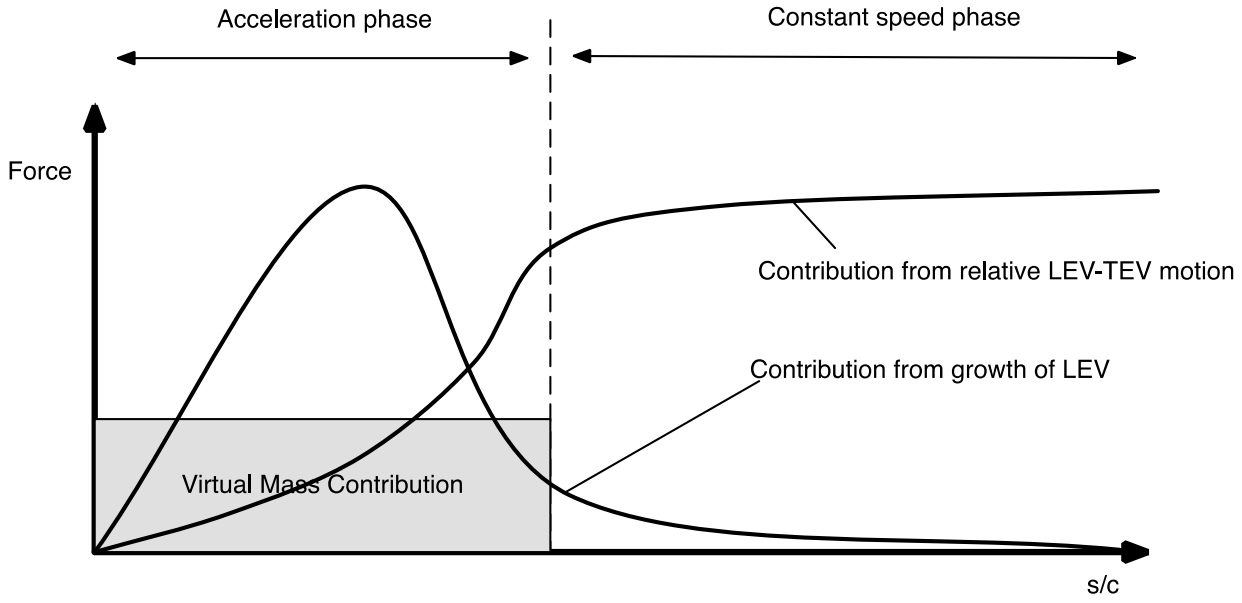

Figure 1-9: Notional Schematic for History of Lift for the Translational Surging Plate, with Contributions During the Phase of Motion where the Plate is Surging (Non-Zero Acceleration) and where the Steady-State Relative Free-Stream Speed has been Attained.

1.4.3 Analytical Derivations for the Pitching Plate

For the pitching plate (Figure 1-10) we again segregate lift into an inertial added mass term, and circulatory contributions. The latter now include a vortex lift term, and an additional contribution due to pitch rate. The latter has the same effect as a bound vortex.

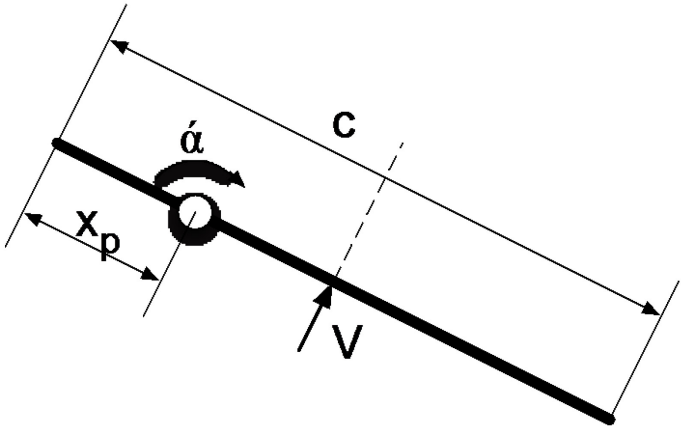

Figure 1-10: Nomenclature for 2D Pitching Plate, with Velocity Normal to the Plate, and Pivot Point Distance from the Leading Edge.

Using the coordinate system in Figure 1-10 we obtain for the normal velocity at the plate's mid-chord:

$$V = \left(\frac{c}{2} - x_p\right)\dot{\alpha}$$

The non-circulatory forces are non-zero only during the smoothing transients of the pitching motion, where the pitch-rate-derivative is non-zero. We can assume the added mass potential flow to be a superposition of a rotation about the mid-chord and a plunge (normal to the plate). The former does not generate a force (but it does generate a moment, which we ignore here). To compute the latter, we once again model the added mass contribution from the equivalent flow of a plate at 90° angle of attack and the mid-chord normal acceleration. Thus the magnitude of the non-circulatory force depends on the hinge location x_p, with rotations about the leading and trailing edges producing spikes of equal opposite magnitudes while rotation about the centre experiences no non-circulatory force. Using the above expression for V and the previously stated equation for the added mass force we obtain for the non-circulatory contribution to lift:

$$C_{L,non-circ} = \frac{\pi c^2}{4U^2}\left(1 - 2\frac{x_p}{c}\right)\ddot{\alpha}$$

Note that the above applies at zero angle of attack. At the end of the pitch (when the second spike appears), the force vector is rotated by α_{end}, thus the second spike is reduced:

$$C_{L,non-circ} = \cos(\alpha_{end})\frac{\pi c^2}{4U^2}\left(1 - 2\frac{x_p}{c}\right)\ddot{\alpha}$$

We next turn to the circulatory contributions. From the pitching motion there is an additional normal velocity V at the mid-chord, which increases the effective angle of attack by approximately V/U_∞. Assuming that this generates additional lift according to $2\pi\alpha$ would give the additional lift contribution (use the result for V derived above; the same result is given by Theodorsen [12]):

$$C_{L,2} = \frac{2\pi}{U_\infty}\left(\frac{c}{2} - x_p\right)\dot{\alpha}$$

However, if we continue to assume that bound circulation due to angle of attack is zero, then the lift contribution due to this additional effective angle of attack should already be included in the vortex lift. We thus propose to ignore this term.

The physical action of pitching the wing does however introduce a real rotation into the fluid. We believe that this is equivalent to a bound circulation (not included in the LEV), and should therefore generate an additional contribution to lift. The existence of this bound circulation can be explained in two ways: either a virtual camber caused by pitch (consider the motion of the TE relative to the LE while the fluid travels along the chord), or an additional circulation due to the plate's rotation (Figure 1-11).

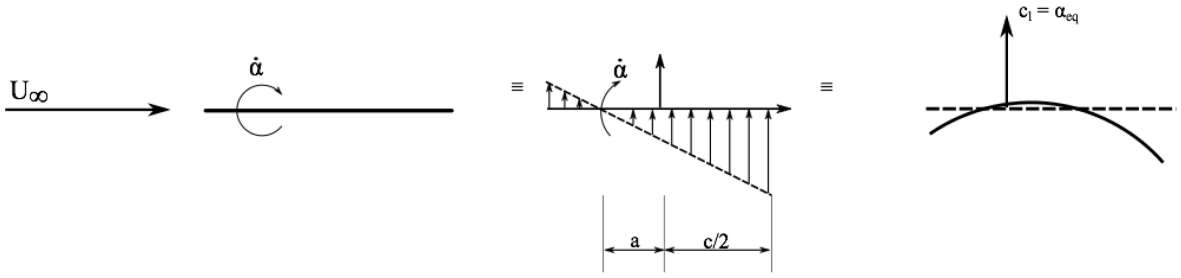

Figure 1-11: Schematic from Classical Unsteady Thin Airfoil Theory, Motivating Quasi-Steady Lift Contribution Due to Pitch; Pitching Produces an Effective Angle of Attack History, or Alternative, an Effective Camber.

Applying unsteady thin airfoil theory [12] to a pitching plate (Figure 1-11) gives the following result for lift coefficient:

$$c_l = 2\pi\left(\alpha + \frac{c\dot{\alpha}}{2U_\infty}\left(\frac{3}{2} - \frac{2x_p}{c}\right)\right)$$

This includes the steady contribution of 2 πα and the above virtual quasi-steady angle of attack. However, after removing both we are left with:

$$c_{l,circ} = \frac{\pi c}{2U_\infty}\dot{\alpha}$$

We can also explain this same result as an additional bound circulation introduced by the speed of rotation, akin to the Magnus effect:

$$\Gamma = \frac{\pi c^2}{4}\dot{\alpha}$$

Then we obtain the above lift contribution by applying $\rho U_\infty \Gamma$. To this we add the circulatory term from LEV and TEV circulation-change and relative displacement, exactly as in the section on the surging plate, except that one must account for the plate's changing incidence-angle during pitch, to isolate the lift component of the vortex-force. The full combination of lift history is schematically presented in Figure 1-12.

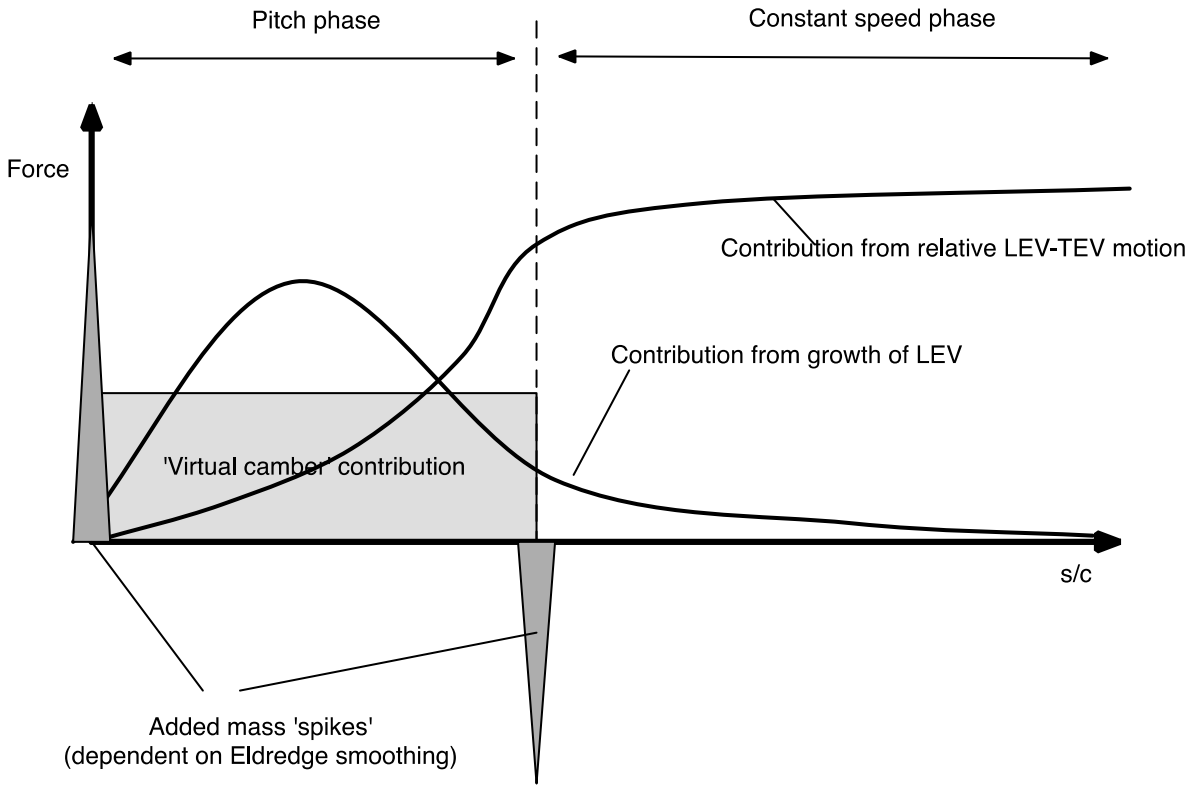

Figure 1-12: Notional Schematic for History of Lift for the Translational Pitching Plate, with Contributions During the Phase of Motion where the Plate is Pitching (Non-Zero Pitch Acceleration is Only During the Smoothing Transients at the Start and End of the Pitching Motion) and After the Final Incidence Angle has been Attained. The relative free-stream speed is assumed to always be constant.

1.5 PARAMETRIC VARIATIONS

The aim behind "canonical cases" is cross-vetting – but the potential parameter space is vast and unwieldy. With not claim of thoroughness, or even of eclectic selection of the most crucial archetypes, we consider the following variations beyond the "canonical":

1) Rectilinear cases were also studied in 2D or nominally in 2D, where the plate spans the test section of a water tunnel. Also, in translation and rotation, different aspect ratios were studied, noting effect of AR on the aerodynamic force coefficient histories, LEV and TEV vortex trajectories and circulation strengths, and spanwise trends therein. For rotational motions, variation of "root cut-out" [13] or the stand-off between the rotational fixed-point and the inboard wingtip could be considered as surrogate for Rossby number, but was not pursued here. The limit of infinite root cut-out in a rotational surge is a rectilinear surge.
2) Variations in Reynolds number, with examination of change in aerodynamic forces and LEV development.
3) Variation of reduced frequency, all the way to infinity (pitch in a zero free stream).
4) Variation of pitch pivot point along the plate's chord.

5) For rectilinear surge we compare linear acceleration profile defined with respect to convective time vs. wall-clock. Further, different smoothing transients are applied to nominally linear ramps defining the acceleration profile. And acceleration profiles can be taken as polynomials of various kind, instead of linear ramps.
6) Plunge resembling pitch.
7) Variations in plate leading edge shape, comparing a square leading edge with sharp corners, to a round leading edge.
8) Variations in peak incidence angle in pitch-ramps, and in the steady incidence angle for a surging-maneuver.

The work described in this Report is meant to be broadly expository, but obviously makes no aspiration to comprehensively cover all pitching/rotating/flapping plate research in the past several years. A good example of work followed by AVT-202, but not reported here, is that of D. Rockwel's group at LeHigh University, which conducted experimental investigations on the flow structure for plates primarily in rotational pitch and rotational surge. Findings for the rotational case include: sensitivity of the leading edge vortex and the overall three-dimensional vortex system to radius of gyration of the plate, which is to say root cut-out; preservation of a highly coherent leading edge vortex to large angles of rotation/travel distance; and preservation of the highly organized structure of the tip vortex-leading edge vortex system on a simultaneously pitching and rotating wing, relative to a purely rotating wing. Meanwhile, for pitching plates in translation, there is an evolution of an "arch vortex", following that originally computed by Visbal [14]. For details, see Refs. [15], [16], [17], [18], [19] and [20].